Eur. Phys. J. B (2015) 88: 211
DOI: 10.1140/epjb/e2015-60234-y

THE EUROPEAN PHYSICAL JOURNAL B

Regular Article

Uncovering transportation networks from traffic flux by compressed sensing

Si-Qi Tang[1,2], Zhesi Shen[1,a], Wen-Xu Wang[1], and Zengru Di[1]

[1] School of Systems Science, Beijing Normal University, Beijing 100875, P.R. China
[2] State Information Center, Beijing 100045, P.R. China

Received 23 March 2015 / Received in final form 8 July 2015
Published online 12 August 2015 –

Abstract. Transportation and communication networks are ubiquitous in nature and society. Uncovering the underlying topology as well as link weights, is fundamental to understanding traffic dynamics and designing effective control strategies to facilitate transmission efficiency. We develop a general method for reconstructing transportation networks from detectable traffic flux data using the aid of a compressed sensing algorithm. Our approach enables full reconstruction of network topology and link weights for both directed and undirected networks from relatively small amounts of data compared to the network size. The limited data requirement and certain resistance to noise allows our method to achieve real-time network reconstruction. We substantiate the effectiveness of our method through systematic numerical tests with respect to several different network structures and transmission strategies. We expect our approach to be widely applicable in a variety of transportation and communication systems.

1 Introduction

Transportation and communication networks are of tremendous importance in modern society, ranging from the Internet to public traffic networks. Since the development of complex network theory [1–3] and the collection of a variety of empirical data, much effort has been dedicated toward understanding traffic dynamics that take place on large transportation networks [4]. Intensive studies have gained insight into the emergence of congestion [5] and relative physical properties, such as phase transition [6]. A large number of routing strategies, as well as structural perturbations, have been presented to prevent the occurrence of congestion and facilitate transmission efficiency [7–9]. It has been realized that network structure plays a prominent role in traffic dynamics. However, due to the evolution of networks to adapt to the increase of traffic demand, most real network structures and link weights continuously change, rendering difficulties in extracting topology. In particular, directly probing links among nodes is infeasible with respect to some networks in the absence of physical connections, such as wireless networks. In this regard, uncovering network structure as an inverse problem from observable data remains outstanding, especially when a small amount of data is available and real-time network inference is necessary.

Solving the problem of network reconstruction based on a detectable time series is of significant interest and wide application, including inferring gene-regulatory networks from gene expression data [10–13], revealing interactions among neurons [14–17] and uncovering social relationships from an individual's behavior for the sake of security. Despite existent methods on network reconstruction, an approach applicable to transportation and communication networks is still lacking. The question related to the inverse problem is this: is it possible to decode the network topology from the recorded traffic flux passing through the port of nodes? This question will become extremely challenging if real-time reconstruction is required based on a small amount of traffic data. Previously proposed methods, which rely on long and continuous time series are no longer valid. To address this issue, an efficient method toward achieving real-time reconstruction is presented.

In this paper, we develop an efficient, data-driven, compressed sensing based approach to infer traffic networks using the data of traffic flux. Compressed sensing theory [18–23], which is subject to convex optimization, was recently developed with the goal of reconstructing sparse signal from rare measurements. The optimization method has been deemed to have wide application in a variety of fields with respect to its sparse data requirement together with high reconstruction accuracy. Although, compressed sensing has been used to uncover the networks of interacting dynamics [24–27], the traffic network system remains intact. We propose a general framework to convert the problem of uncovering traffic networks into the sparse-signal reconstruction, which enables the use of compressed sensing theory. Specifically, we assume to be able to record the incoming and outgoing flux at the port

[a] e-mail: shenzhesi@mail.bnu.edu.cn

of each node at different times. We will demonstrate that the network structure of transportation networks can be efficiently and precisely inferred based on a relatively small amount of traffic flux data compared to the network size. We substantiate our method by taking three transmission models into account: broadcast model [7], local routing strategy model [8] and global routing strategy model [9].

2 Methods

2.1 Packets transmission model

Broadcast model (BM) is often used for modeling the broadcast procedure in communication networks, such as the Internet and wireless networks [7]. In this model, each node broadcasts the copies of information stored in its queue to all its neighbors.

Local routing model (LRM). Packets are routed based only on local topological information with a single tunable parameter α. When delivering packets, each node will do a local search among its neighbors and deliver the packet directly to its target if its destination is found within the searched area. Otherwise, the packet will be delivered to a node i, one of the neighbors of the searching node, according to the preferential probability:

$$\Theta_{ji} = \frac{k_i^\alpha}{\sum_{l\in\Gamma_j} k_l^\alpha}, \tag{1}$$

where Γ_j is the neighbor set of j, k_i is the degree of node i and α is an adjustable parameter. When α is above 0, large degree nodes are preferred; below 0, small degree nodes are preferred. Θ_{ji} represents the probability that one data packet is delivered from node j to node i if i is not its destination.

Global routing model (GRM). Each packet is navigated according to the weighted shortest path between its source and destination. The weight of the link between node i and node j is $w_{ij} = (k_i k_j)^\lambda$, where k_i refers to the degree of node i and λ is an adjustable parameter that represents the routing strategy. By recording all the shortest paths between each pair of nodes, we can obtain a fixed routing table for the traffic system. There may be more than one shortest path between two nodes; in this case, one of the paths will be randomly chosen. All packets follow the fixed routing table during the transmission simulation processes.

The data of traffic flux are acquired from simulations of the three traffic models. In each model, data packets are randomly generated with randomly chosen sources and destinations at each time step. For a given node, all packets will be delivered to its neighbors, according to the routing strategy at one step in the absence of congestion and transmission delay. There are two types of flow, the incoming flow and the outgoing flow at each node, which can be measured by detecting the port of nodes (e.g., routers and hubs). Due to the preference of packets delivered in the GRM, only the flow of recently generated packets are recorded.

2.2 Compressed sensing theory

The general problem that compressed sensing theory addressed can be described as reconstructing a sparse vector $\mathbf{X} \in R^N$ from linear measurements $\mathbf{Y}$ associated with $\mathbf{X}$ in the form

$$\mathbf{Y} = \Phi \cdot \mathbf{X}, \tag{2}$$

where $\mathbf{Y} \in R^M$ and Φ is an $M \times N$ matrix. The striking property of compressed sensing is that, if Φ satisfies the restricted isometry property [18–23], the number of required data to reconstruct $\mathbf{X}$ can be much less than the length of signal vector $\mathbf{X}$, i.e., $M \ll N$. Accurate reconstruction can be realized by means of solving the following optimization problem [18–23]:

$$\min ||\mathbf{X}||_1 \text{ s.t. } \mathbf{Y} = \Phi \cdot \mathbf{X}, \tag{3}$$

where $\min ||\mathbf{X}||_1 = \sum_{i=1}^N |\mathbf{X}_i|$ is the L_1 norm of vector $\mathbf{X}$. Solutions of the convex optimization problem have been worked out in recent years [18–23].

2.3 Reconstruction framework

Establishing the relation between the reconstructing problem and equation (2) can be achieved by considering the flux conservation between incoming and outgoing flows. For an arbitrary node i, the incoming flux $F_i^{\text{in}}(t)$ from other nodes at time t is

$$F_i^{\text{in}}(t) = \sum_{j=1, j\neq i}^{N} F_j^{\text{out}}(t) X_{i,j}(t), \tag{4}$$

where $F_j^{\text{out}}(t)$ is the outgoing flux of j and $X_{i,j}(t)$ represents the proportion of flux from node j to node i in $F_j^{\text{out}}(t)$ at time t.

Due to the characteristic difference between the local routing model and the global routing model, the expression of $X_{i,j}(t)$ varies a little; thus we treat them separately. For the LRM, the proportion $X_{i,j}(t)$ of an arbitrary node i from node j at time t is

$$X_{i,j}(t) = \frac{k_i^\alpha}{\sum_{p\in\Gamma_j} k_p^\alpha} a_{ij}, \tag{5}$$

where a_{ij} stands for the elements of the adjacency matrix ($a_{ij} = 1$ if i connects to j and $a_{ij} = 0$ otherwise). For a given network topology and parameter α, the proportion $X_{i,j}(t)$ is time-invariant. By substituting equations (5) and (4) can be rewritten as:

$$F_i^{\text{in}}(t) = \sum_{j=1, j\neq i}^{N} F_j^{\text{out}}(t) \frac{k_i^\alpha}{\sum_{p\in\Gamma_j} k_p^\alpha} a_{ij}. \tag{6}$$

If measurements at different times $t = t_1, t_2, \ldots, t_m$ are available, equation (6) can be written in the matrix form $\mathbf{Y}_i^{m\times 1} = \Phi_i^{m\times(N-1)} \cdot \mathbf{X}_i^{(N-1)\times 1}$, where

$$\mathbf{Y}_i = \left[F_i^{\text{in}}(t_1), F_i^{\text{in}}(t_2), \ldots, F_i^{\text{in}}(t_m)\right]^{\text{T}}$$

is the incoming flux vector of i,

$$\Phi_i = \begin{pmatrix} F_1^{\text{out}}(t_1) & \dots & F_{i-1}^{\text{out}}(t_1) & F_{i+1}^{\text{out}}(t_1) & \dots & F_N^{\text{out}}(t_1) \\ F_1^{\text{out}}(t_2) & \dots & F_{i-1}^{\text{out}}(t_2) & F_{i+1}^{\text{out}}(t_2) & \dots & F_N^{\text{out}}(t_2) \\ \vdots & \vdots & \vdots & \vdots & \vdots & \vdots \\ F_1^{\text{out}}(t_m) & \dots & F_{i-1}^{\text{out}}(t_m) & F_{i+1}^{\text{out}}(t_m) & \dots & F_N^{\text{out}}(t_m) \end{pmatrix}, \tag{7}$$

is the outgoing flux matrix and

$$\mathbf{X}_i = \left[\frac{k_i^\alpha}{\sum_{p\in\Gamma_1} k_p^\alpha} a_{i1}, \frac{k_i^\alpha}{\sum_{p\in\Gamma_2} k_p^\alpha} a_{i2}, \dots, \frac{k_i^\alpha}{\sum_{p\in\Gamma_N} k_p^\alpha} a_{iN} \right]^{\mathrm{T}}.$$

The vector $\mathbf{Y}_i$ and the matrix Φ_i can be constructed immediately from the detectable traffic flux, and the vector $\mathbf{X}_i$ to be reconstructed is sparse, rendering applicable the compressed sensing method. As a result, we can exactly reconstruct all neighbors of node i from relatively small amounts of measurements. In a similar way, the neighboring vectors of all nodes can be uncovered and the whole network structure can be obtained by matching the neighboring sets of all nodes.

As for the broadcast model, at each step, each node broadcasts the exact copies of the packets stored in its queue to its neighbors. Thus, we can treat it as a special case of the local routing model in which α is 0, that is, $X_{i,j} = \frac{1}{k_j}$.

Meanwhile, for the global routing model, all packets are transferred according to a routing table. Therefore, once the routing table is determined, the path of a randomly generated packet to its destination is fixed. For a certain number of packets generated at node i with random destinations, the ratio of data transferred from i to one of its neighbors, e.g. j, denoted as Π_{ij}, is time-invariant. Thus, similar to the local routing model, we have the same matrix Φ and vector $\mathbf{Y}_i$, and the vector $\mathbf{X}_i$ becomes

$$\mathbf{X}_i = [\Pi_{1i}a_{i1}, \dots, \Pi_{i-1,i}a_{i,i-1}, \Pi_{i+1,i}a_{i,i+1}, \dots, \Pi_{Ni}a_{iN}]^{\mathrm{T}}.$$

3 Results

3.1 Reconstructing networks

To quantify the validity and efficiency of our compressed sensing based framework for inferring transportation networks in terms of the number of measurements, we study the success rate of existent links (SREL) and null connections (SRNC), which correspond to non-zero and zero element values in the adjacency matrix, for homogeneous and heterogeneous network structures, including random [28], small-world [29] and scale-free [30]. Because the reconstruction method is implemented for each node in the network, we define SREL and SRNC on the basis of each individual node, and the two success rates for the entire network are the respective averaged values over all nodes. The length of a time series is represented by the number of recorded flux data during the traffic dynamics normalized by the network size N (data $\equiv M/N$). As shown in Figure 1a, at data = 0.4, there is a vast gap between the reconstructed $X_{i,j}$ corresponding to the existent links (green points in Fig. 1a) and null connections (yellow points in Fig. 1a) of all nodes, enabling us to correctly identify all links by simply setting a threshold within the gap. All the reconstructed values that are larger than the threshold correspond to links; otherwise, $X_{i,j}$'s are deemed null connections. Obviously, the success rate of this method depends on how we choose an appropriate threshold. Here, we first draw a histogram distribution of elements in the reconstructed vector $\mathbf{X}_i$ (e.g., Fig. 1b), and then select as the threshold the location at which the vertical value of the distribution becomes zero for the first time from the right side of the highest peak.

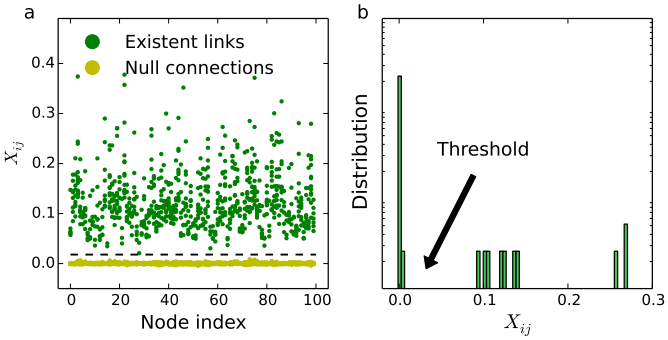

Fig. 1. (a) Reconstructed values of elements in $\mathbf{X}$ for LRM on ER random network at data = 0.4. (b) Histogram of the reconstructed values of X_i for Node 19 shown in (a). The number of nodes is $N = 100$ and the average node degree is $\langle k \rangle = 8$.

The success rates of reconstructions for three types of traffic models and three types of network structures are shown in Figure 2. For all studied combinations of dynamics and networks, full reconstruction can be achieved with quite low amounts of data. For instance, for random and small-world networks, a 100% success rate can be achieved insofar as the data amount exceeds a critical value between 0.3 and 0.4. This critical value is approximately 0.5 for scale-free networks, slightly larger than for the homogeneous networks. This can be attributed to the presence of hubs, the connections of which are relatively much denser than other nodes. In general, we found that a lower amount of data is required when the reconstructed vector is sparser. Therefore, heterogeneous networks usually need more data to handle hubs to accomplish complete reconstruction, compared to homogeneous networks.

In real systems, noise or error in the data record is inevitable. Regarding this, we test the robustness of our method against additive noise involved in the measurements of traffic flux. Particularly, white Gaussian noise is added to the time series of the recorded traffic flux. To measure the power of the noise, we introduce the signal-to-noise ratio (SNR), a measure used to compare the degree of a desired signal to the degree of background noise [31]. The expression of SNR is defined in a logarithmic decibel

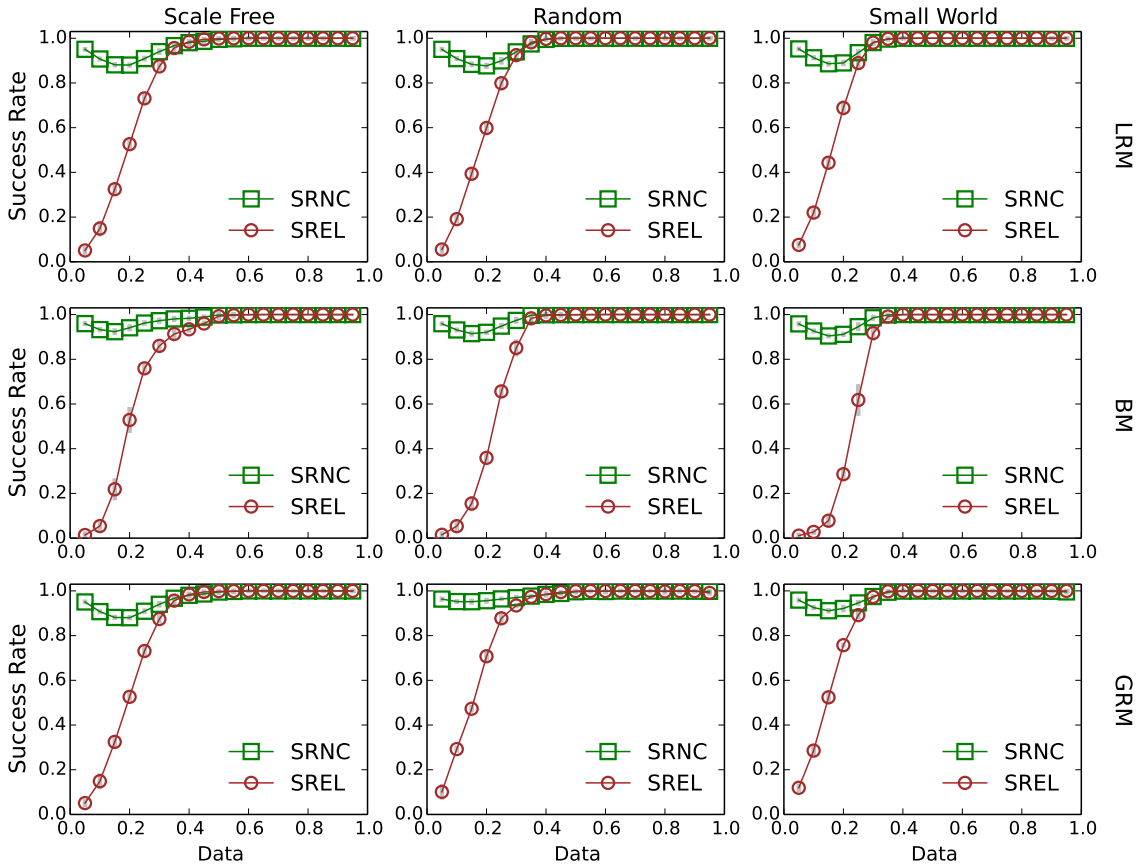

Fig. 2. Success rates of inferring three types of networks: scale-free, random and small-world for LRM, BM and GRM dynamics. The network size N is 100 and the average degree $\langle k \rangle$ is 8. Each data point is obtained by averaging over 10 independent realizations. For each realization, measurements are randomly picked from a time series of incoming and outgoing flux. We set $\alpha = 1$ for LRM and $\lambda = 0$ for GRM, respectively.

scale as,

$$\mathrm{SNR}_{\mathrm{dB}} = 10\log_{10}\left(\frac{P_{\mathrm{signal}}}{P_{\mathrm{noise}}}\right), \tag{8}$$

where P_{signal} refers to the average power of the signal and P_{noise} is the average power of the noise. This means that the smaller the value of SNR is, the larger the ratio of the noise is. In our application, the measured flow data are considered as the signal, then the different intensities of noise are added. The reconstruction performance against different SNRs is shown in Figure 3. We can see from the figure that the success rate can rise to nearly 1 when the power of the signal exceeds a critical value between 40 dB and 50 dB.

3.2 Inferring routing parameters

Having successfully reconstructed the network structure, we can estimate the routing parameters of the local and global routing models. Here, we offer an effective method to infer the routing parameters solely on the recorded traffic flux. In particular, after all links have been successfully estimated, α and λ can be deduced from the relations between node degrees and traffic flux.

3.3 Inferring local routing parameter α

The relation between the incoming flux of node i and k_i is given by the mean field approximation [32]:

$$F_i^{\mathrm{in}} \sim k_i^{\alpha+1}. \tag{9}$$

Therefore, by fitting the relation between F_i^{in} and k_i in the log-log form, we can estimate the parameter α.

Figure 4 shows the linear relations between node degrees and incoming flux in a log-log scale under different values of the local routing parameter α, which can be explained via mean field approximation [32]. The parameters α of the local routing model on different networks are in quite good agreement with the true values with small prediction errors, as shown in Figure 5. For random and small-world networks, most of the boxes are on the line; only when the absolute value of α is large do some boxes slightly deviate from the line. This is because, for large α, the mean field approximation works does not work as well as when α is small, especially in scale-free networks.

3.4 Inferring global routing parameter λ

Unlike the simple relation between α and the slopes of fitting curves in the local routing model, the global routing

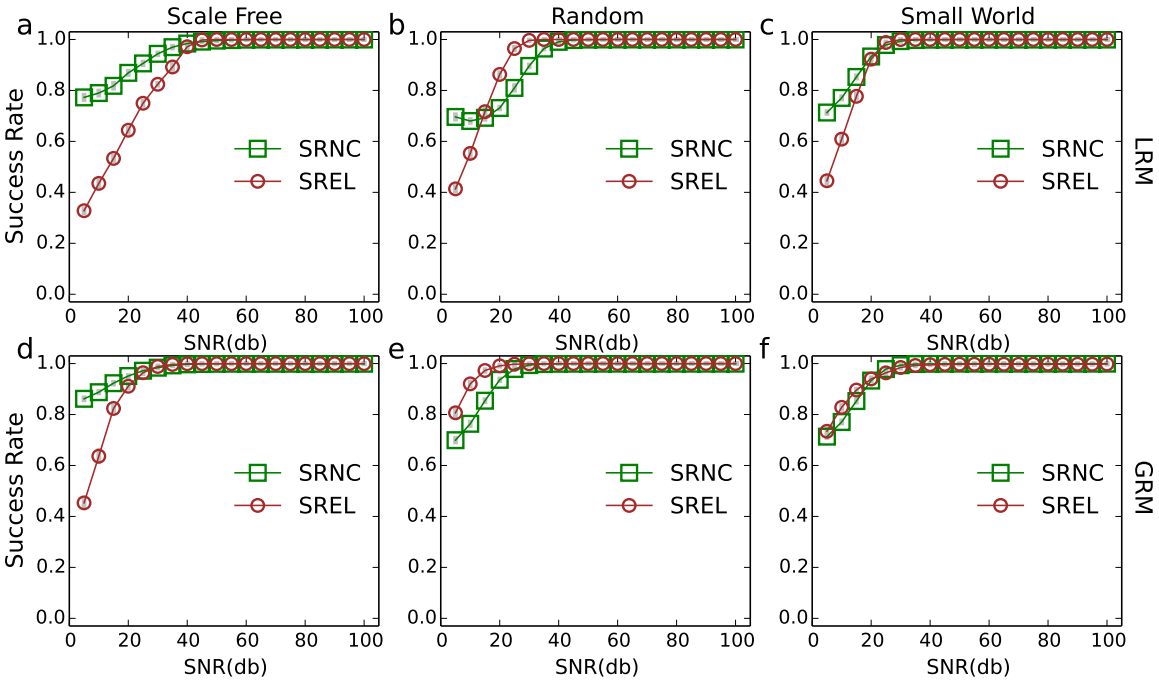

Fig. 3. Noise immunity of reconstructing three types of networks for LRM (a)–(c) and GRM (d)–(f). The average node degree is $\langle k \rangle = 8$ and the routing parameters are $\alpha = 1$ for LRM and $\lambda = 0$ for GRM.

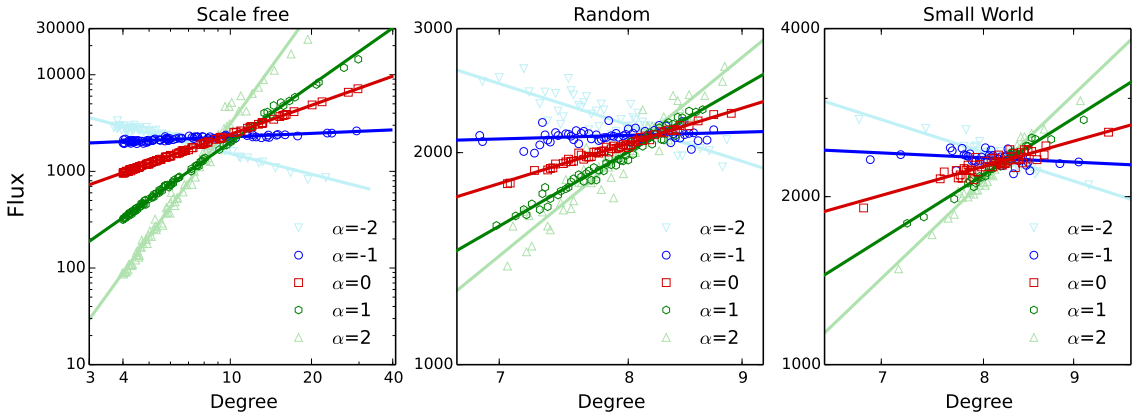

Fig. 4. Least square fitting curve of node degrees and the corresponding traffic flux for the local routing model on three types of networks under different values of α. Each data point for curve fitting is averaged over 20 independent realizations. The network size N is 100, and the average degree $\langle k \rangle = 8$.

model presents a more complex relation between the values of the routing parameter λ and the slopes of the fitting lines.

To estimate the value of parameter λ used in the simulations, we test a certain range of λ and obtain the slope of the corresponding fitting line between the traffic flux and node degree in log-log coordinates. Then, we draw the interpolation fitting curve of the node degree and traffic flux as the baseline shown in Figure 6. After fully reconstructing the network structure, we can use the estimated node degree and the observed incoming flux of each node to draw a fitting curve in log-log coordinates; thus, we can obtain the slope of the fitting curve, which correspond to the vertical axis value in Figure 6, and then the predicted global routing parameter.

The box plots in Figure 7 show the accuracy of our method. Each box contains 50 independent simulations for the corresponding parameter and the line that gets through is $\hat{\lambda} = \lambda$. The results are relatively accurate for random and small-world networks, as most of the boxes are on the line. For a scale-free network, the result is not so ideal for large values of parameter λ when considering the failure of the mean field approximation. Therefore, the routing strategy parameters of heterogeneous networks are usually hard to determine, compared to homogeneous networks when the link weight parameter becomes large.

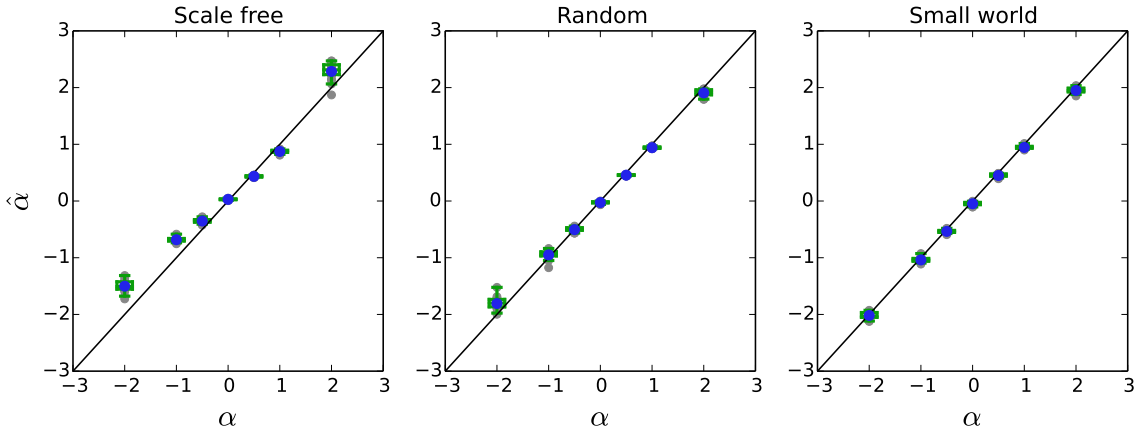

Fig. 5. Box plots for predicted LRM parameter on three types of networks, each box contains 20 independent simulations. The horizontal axis is the true parameter α used in simulations and the vertical axis is the estimated $\hat{\alpha}$. The blue line is $\hat{\alpha} = \alpha$.

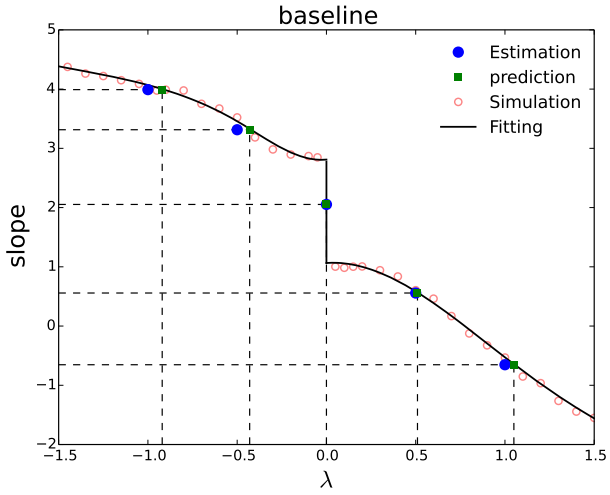

Fig. 6. Baseline for estimating the routing parameter though the predicted result. This is one realization of a random network with $N = 100$ and $\langle k \rangle = 8$; the red spots are from the tested λ in interval $[-1.5, 1.5]$, the black line is the interpolation curve, the blue spots are the fitting slopes of uncovered node degrees and the corresponding traffic flux, and the green squares are the corresponding values of the predicted results, whose horizontal axis values are the uncovered parameter λ.

So far, we have successfully inferred the network structure and the routing strategy parameters from the measured flux data; this enables us to not only find the adjacency connections of nodes, but also the routing strategy. It is of great significance that this method enables us to deep mine the information of a network and its dynamics process.

4 Discussion

In this study, we developed a general approach to uncover transportation and communication networks from a relatively small amount of traffic flux data. The key of our method lies in casting the inverse problem into the problem of sparse-signal reconstruction, which can be addressed with the aid of compressed sensing theory. Due to the property of compressed sensing, our method possesses the advantages of sparse data requirement and high inferring accuracy, which benefits the real-time inference of traffic networks. Our method is validated by considering different types of network structure and three transmission models. Our approach is a necessary stepping stone towards efficiently inferring various real traffic networks based on observable traffic flux data. Because of the importance and ubiquity of modern traffic networks, our method is of great significance and may have potential applications in a variety of systems.

It is noteworthy that to ensure sparse data requirement by using the compressed sensing, matrix Φ should satisfy the restricted isometry property (RIP) [19]. However, for an arbitrary matrix, the test of RIP is an NP-hard problem [33], rendering the test computational prohibitive. At present, only a few types of matrices have been proved to have RIP, e.g., Gaussian random matrix, and the RIP test of our compressed-sensing based reconstruction remains elusive. Nevertheless, our method is still quite successful, which lies in the presence of sufficient randomness in matrix Φ. In general, in a complex networked system, such as in the traffic network, nonlinear properties and noise give rise to random fluctuations in the time series of flux. Moreover, because that matrix Φ is constructed from the time series, Φ is sufficiently random. In analogy with the Gaussian random matrix, the randomness in Φ accounts for the requirement of small amounts of data. Thus, though the RIP is hard to be rigorously ensured, our approach still has practical significance for reconstructing real networked systems in an extremely sufficient and accurate manner.

This work is supported by the National Natural Science Foundation of China under Grant Nos. 11105011 and 61374175, the Beijing Nova program and the Foundation Research Funds for the Central Universities.

All authors contributed equally to the paper.

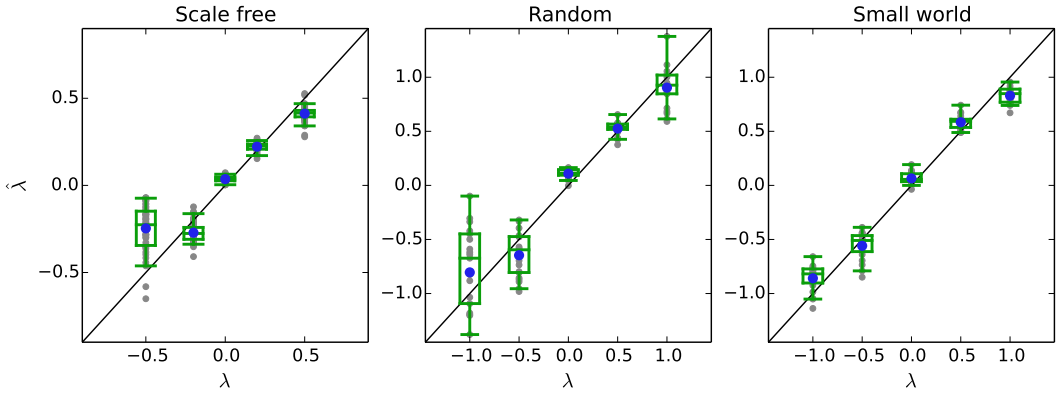

Fig. 7. Box plots for the predicted GRM parameters of three types of networks; each box contains 20 pieces of simulation data. The horizontal axis is the true parameter λ used in simulations and the vertical axis is the estimated $\hat{\lambda}$. The blue line is $\hat{\lambda} = \lambda$.

References

1. A.-L. Barabási, Nat. Phys. **1**, 68 (2005)
2. S. Boccaletti, V. Latora, Y. Moreno, M. Chavez, D.-U. Hwang, Phys. Rep. **424**, 175 (2006)
3. M. Newman, *Networks: An Introduction* (Oxford University Press, 2010)
4. D. Li, B. Fu, Y. Wang, G. Lu, Y. Berezin, H.E. Stanley, S. Havlin, Proc. Natl. Acad. Sci. USA **112**, 669 (2014)
5. W.-X. Wang, Z.-X. Wu, R. Jiang, G. Chen, Y.-C. Lai, Chaos **19**, 033106 (2009)
6. B.-H. Wang, W.-X. Wang, Pramana **71**, 353 (2008)
7. D. Li, X. Jia, H. Liu, IEEE Trans. Mobile Computing **3**, 144 (2004)
8. W.-X. Wang, B.-H. Wang, C.-Y. Yin, Y.-B. Xie, T. Zhou, Phys. Rev. E **73**, 026111 (2006)
9. G. Yan et al., Phys. Rev. E **73**, 046108 (2006)
10. T.S. Gardner, D. di Bernardo, D. Lorenz, J.J. Collins, Science **301**, 102 (2003)
11. M. Bansal, V. Belcastro, A. Ambesi-Impiombato, D. di Bernardo, Mol. Syst. Biol. **3**, 78 (2007)
12. F. Geier, J. Timmer, C. Fleck, BMC Syst. Biol. **1**, 11 (2007)
13. M. Hecker, S. Lambeck, S. Toepferb, E. van Someren, R. Guthke, BioSystems **96**, 86 (2009)
14. S. Grün, M. Diesmann, A. Aertsen, Neural Comput. **14**, 43 (2002)
15. R. Gütig, A. Aertsen, S. Rotter, Neural Comput. **14**, 121 (2002)
16. G. Pipa, S. Grün, Neurocomputing **52-54**, 31 (2003)
17. K. Supekar, V. Menon, D. Rubin, M. Musen, M.D. Greicius, PLoS Comput. Biol. **4**, e1000100 (2008)
18. E.J. Candès, J. Romberg, T. Tao, IEEE Trans. Inf. Theor. **52**, 489 (2006)
19. E.J. Candès, J.K. Romberg, T. Tao, Commun. Pure Appl. Math. **59**, 1207 (2006)
20. D.L. Donoho, IEEE Trans. Inf. Theor. **52**, 1289 (2006)
21. R.G. Baraniuk, IEEE Sig. Proc. Mag. **24**, 118 (2007)
22. E.J. Candès, M.B. Wakin, IEEE Sig. Proc. Mag. **25**, 21 (2008)
23. J. Romberg, IEEE Sig. Proc. Mag. **25**, 14 (2008)
24. W.-X. Wang, R. Yang, Y.-C. Lai, V. Kovanis, C. Grebogi, Phys. Rev. Lett. **106**, 154101 (2011)
25. W.-X. Wang, Y.-C. Lai, C. Grebogi, J. Ye, Phys. Rev. X. **1**, 021021 (2011)
26. Z. Shen, W.-X. Wang, Y. Fan, Z. Di, Y.-C. Lai, Nat. Commun. **5**, 1 (2014)
27. X. Han, Z. Shen, W.-X. Wang, Z. Di, Phys. Rev. Lett. **114**, 208701 (2015)
28. P. Erdös, A. Rényi, Publ. Math. Debrecen **6**, 290 (1959)
29. D.J. Watts, S.H. Strogatz, Nature **393**, 440 (1998)
30. A.-L. Barabási, R. Albert, Science **286**, 509 (1999)
31. D.J. Schroeder, in *Astronomical Optics*, 2nd edn. (Academic Press, 2009), p. 443
32. H. Zhang, Z. Liu, M. Tang, P.M. Hui, Phys. Lett. A **364**, 177 (2007)
33. A.M. Tillmann, M.E. Pfetsch, IEEE Trans. Inf. Theor. **60**, 1248 (2014)